

# Automated Complex Permittivity Characterization of Ceramic Substrates Considering Surface-Roughness Loss

A. Ege Engin\* and Pavithra Pasunoori

**Abstract**—This paper presents a new method to extract the frequency-dependent dielectric constant and loss tangent of ceramic substrates from high frequency measurements of cavity resonators. A cavity resonator can be realized using two ground planes connected with vias to form the side walls. Recently, a rapid plane solver has been developed to efficiently and accurately simulate cavity resonators and extract materials properties by manually fitting simulations to measurements. In this paper, we demonstrate how the fitting process can be automated. In order to extract the dielectric constant and loss tangent, many simulations need to be run to find the parameters that provide the best match with the measurements. This is a computationally expensive approach. We will present a new method based on tracking sensitivity, which provides a parameterized macromodel for the resonators. Using this approach, the simulation data can be expressed as a low-order rational function of the complex permittivity. Hence, varying the complex permittivity to find the best fit can be done in negligible time after the macromodel has been generated. This new method will be applied to extract the dielectric constant and loss tangent of a ceramic substrate in the presence of surface roughness loss.

**Keywords**—Dielectric constant, HTCC, loss tangent, materials characterization, tracking sensitivity, surface roughness

## INTRODUCTION

Cavity resonators can be realized easily using ground planes and vias. Due to the high-Q nature of a cavity resonator that does not suffer from radiation losses, it is an excellent candidate for characterization of the dielectric constant and loss of ceramic substrates. The advantages of using a cavity resonator for materials characterization compared with a standard transmission-line based approach can be summarized as: (a) elimination of the contribution of radiation losses to the extracted loss; (b) relative insensitivity of the extracted parameters to technological tolerances such as variability in conductor width and spacing due to copper etching; and (c) extraction of the parameters of a homogeneous dielectric medium (in other words, no air-dielectric interface as in a microstrip line).

Many techniques are available to characterize the material properties using transmission-line based methods, such as the short-pulse propagation technique based on time-domain reflectometry measurements [1], frequency-domain characterization of microstrip lines [2], microstrip bandpass filters [3], coupled

microstrip resonators [4], or microstrip gap or ring resonators [5-7]. A survey of commonly used techniques for characterization of PCB dielectrics is provided in [8].

Fig. 1 shows the sketch of a cavity resonator. A large number of vias should be used in order to reduce the inductance of the vias and obtain an accurate electric wall boundary. The advantages of using cavity resonators in materials characterization to eliminate radiation losses and fringe fields have been demonstrated [9-11]. In the classical method, an analytical equation is used to estimate the permittivity at resonance frequencies of a resonator (of size  $a \times b$ ) as

$$\epsilon = \frac{1}{4f_c^2 \mu} \left[ \left( \frac{m}{a} \right)^2 + \left( \frac{n}{b} \right)^2 \right] \quad (1)$$

at the discrete resonance frequency  $f_c$  of the  $TM_{mn0}$  mode of the resonator. In eq. (1),  $\mu$  is the permeability of the dielectric material, which is typically equivalent to the free space permeability for packages and printed circuit boards. This equation is accurate for negligible conductor losses; hence, it becomes inaccurate at higher frequencies. Also, the resonance frequency changes depending on the location of the probes (Port 1 and Port 2) [12]. Eq. (1) is based on a rectangular waveguide resonator with open boundaries used in the full-sheet resonance method (e.g., [12-15]). A similar methodology is based on the measurement of a circular shaped resonator at its center [16]. It has been shown in [10] that the contribution of the fringe fields and radiation losses can be substantial and affect the extracted parameters. Hence, in this paper we use cavity resonators (i.e., resonators with shorted boundaries as in Fig. 1) and a rapid electromagnetic solver for cavity resonators following [10].

In [10], dielectric material properties are extracted by manually overlapping simulation results with measured results. This is a computationally expensive approach and prone to user error. We will present a new method based on tracking sensitivity, which was originally proposed for power and ground planes [17], and later used to obtain a parameterized macromodel for cavity resonators [18]. Using this approach, the simulation data can be expressed as a low-order rational function of the complex permittivity. Hence, varying the complex permittivity to find the best fit can be done in negligible time after the macromodel has been generated. As a result, an efficient automated methodology can be developed. However, the extracted loss tangent for low loss materials will be inaccurate if conductor surface roughness loss is not considered. In this paper, we extend our previous methodology in [17] and

Received August 1, 2012; Revised October 20, 2012; Accepted October 30, 2012  
Department of Electrical and Computer Engineering, San Diego State University, San Diego, California, 92182

\*Corresponding author; email: aengin@mail.sdsu.edu

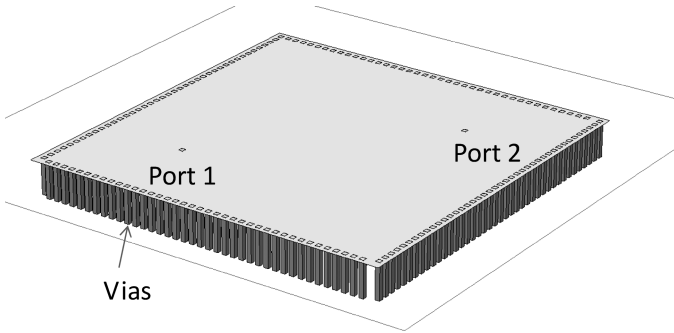


Fig. 1. Cavity resonator used for characterization of the dielectric constant and loss tangent.

[18] by including the surface roughness loss. We also apply the methodology for the first time on a ceramic material.

### CURVE FITTING SIMULATIONS TO MEASUREMENTS

Our methodology is based on the simulation of the cavity resonators using a rapid plane solver and creation of a macromodel using the tracking sensitivity algorithm. Details of these algorithms can be found in [10], [17], and [18]. As a result of the tracking sensitivity algorithm, the input and transfer impedances of the cavity resonator are available as a rational function in the form of

$$Z = \sum_{j=1}^k \frac{f_j}{1 - \Delta\epsilon\lambda_j} \quad (2)$$

where  $k$  is the order of the model and the variables  $f_j$  and  $\lambda_j$  are obtained following the tracking sensitivity algorithm. Note that these coefficients need to be computed separately at each frequency point. Using our methodology, it is possible to quickly recalculate the impedance parameters for a slight change in the complex relative permittivity by  $\Delta\epsilon$ , instead of using the rapid solver starting from scratch. Hence, this greatly improves the simulation speed for an iterative algorithm that

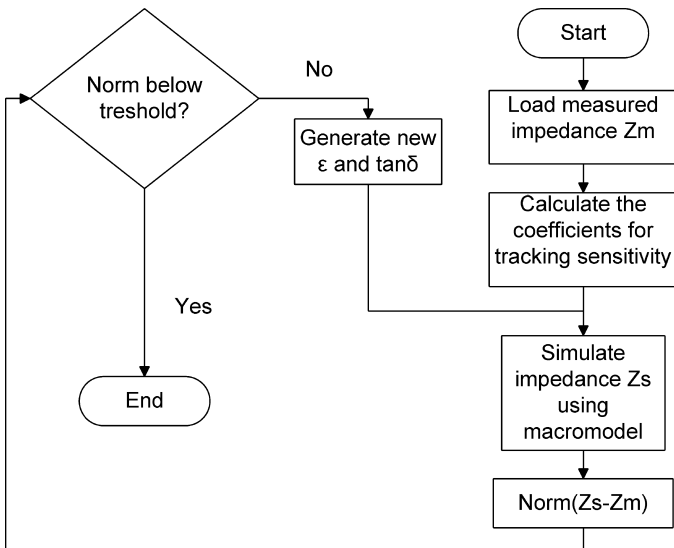


Fig. 2. Flow chart for curve-fitting simulations to measurements.

finds the optimum value of  $\Delta\epsilon$  for the best fit between simulations and measurements.

Fig. 2 shows a flow chart for fitting the simulation results to measured data. The simulated impedances  $Z$  are calculated using the rational function or macromodel in eq. (2). The nonlinear curve-fitting problem is solved in the least-squares sense.

### CHARACTERIZATION OF HTCC CERAMIC

The AO630 high temperature cofired ceramic (HTCC) from Kyocera was characterized using shorted resonators of two different sizes. The larger resonator was  $928 \text{ mil} \times 928 \text{ mil}$ , while the smaller resonator was  $278 \text{ mil} \times 278 \text{ mil}$ . The two ports were placed one-fourth of a diagonal away from two opposite corners of the resonator. After measurements, cross sections were taken to obtain accurate dielectric thicknesses and surface roughness rms values. A picture of the fabricated resonators and the cross section is shown in Fig. 3. The vias on the boundaries of the resonators should be placed closer than one-tenth of a wavelength to achieve a continuous electric wall. The shape of the via is not critical. However, the via clearances required for probing (as shown in Fig. 3) should be much smaller than the cavity dimensions in order to maintain a solid cavity resonator. Therefore, very small cavity resonators are not recommended.

The two-port S-parameters were measured using a vector network analyzer and  $250\text{-}\mu\text{m}$  GSG probes. The measurements were taken after an SOLT calibration. The transfer impedance was then obtained from the calibrated S-parameters. In the simulations, a discretization of 64 unit cells in each direction was used. After cross-sectioning, the dielectric thickness of the large resonator was measured as  $180 \mu\text{m}$ , whereas the small resonator's thickness was  $188 \mu\text{m}$ . The rms value of surface roughness was measured as  $0.6 \mu\text{m}$ . The conductor is copper based, but is not pure copper. A conductivity of  $\sigma_c = 3 \times 10^7 \text{ S/m}$  was assumed in the simulations. There is no general way of separating the conductor losses from dielectric losses through high frequency measurements. Hence, the extracted loss tangent will in general depend on the assumed surface roughness and conductivity of the conductor. Therefore, accurate loss

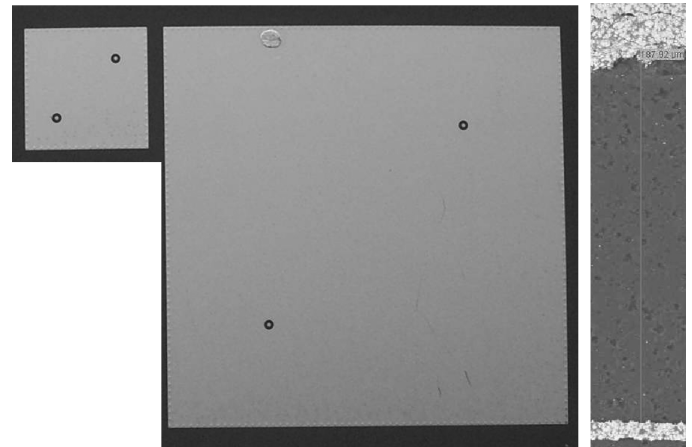


Fig. 3. Left: small resonator of size  $278 \text{ mil} \times 278 \text{ mil}$ ; center: large resonator of size  $928 \text{ mil} \times 928 \text{ mil}$ ; right: cross section of the small resonator showing a dielectric thickness of  $188 \mu\text{m}$ .

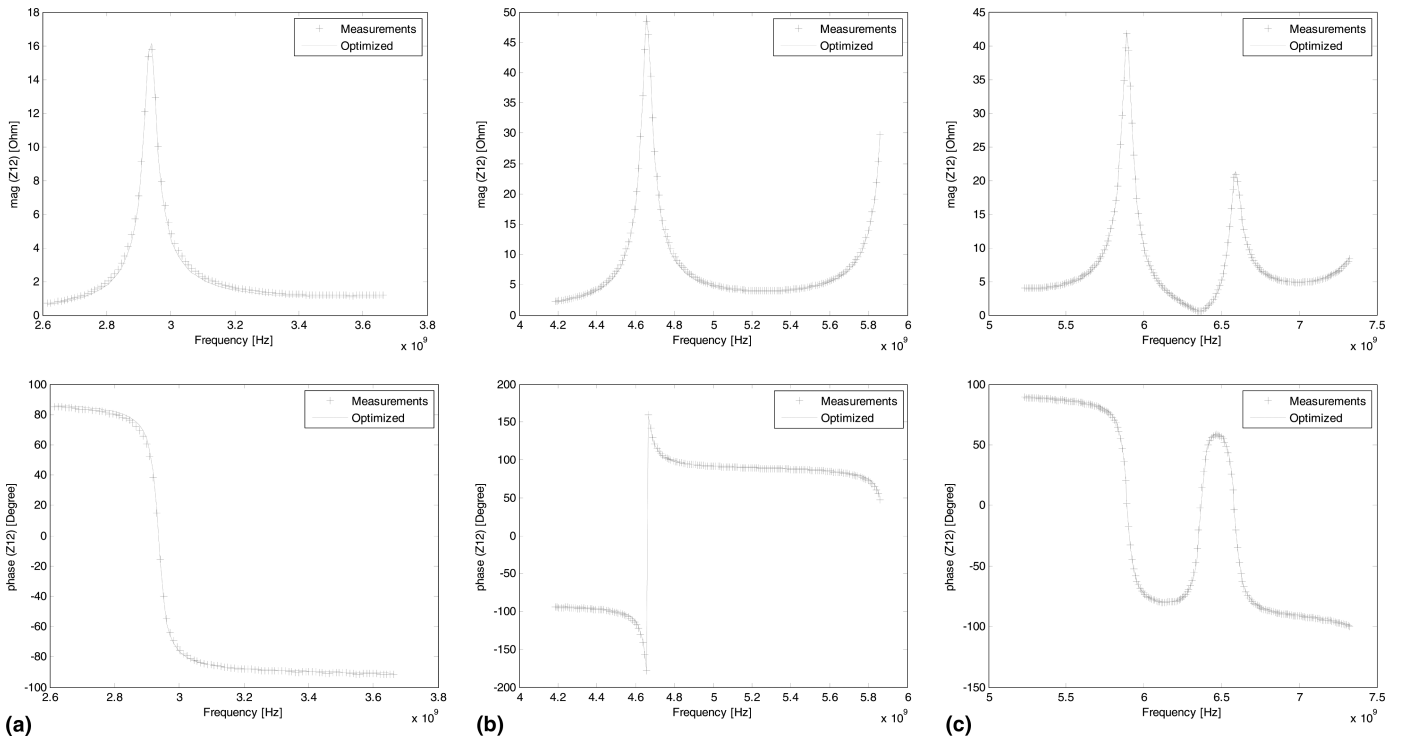


Fig. 4. Large resonator (928 mil × 928 mil): Measurement results versus fitted simulations at (a) the first, (b) the second, and (c) the third and fourth resonance frequencies. Nominal value used:  $\epsilon_r = 9$ ,  $\tan\delta = 0.002$ . Extracted values are shown in Fig. 6.

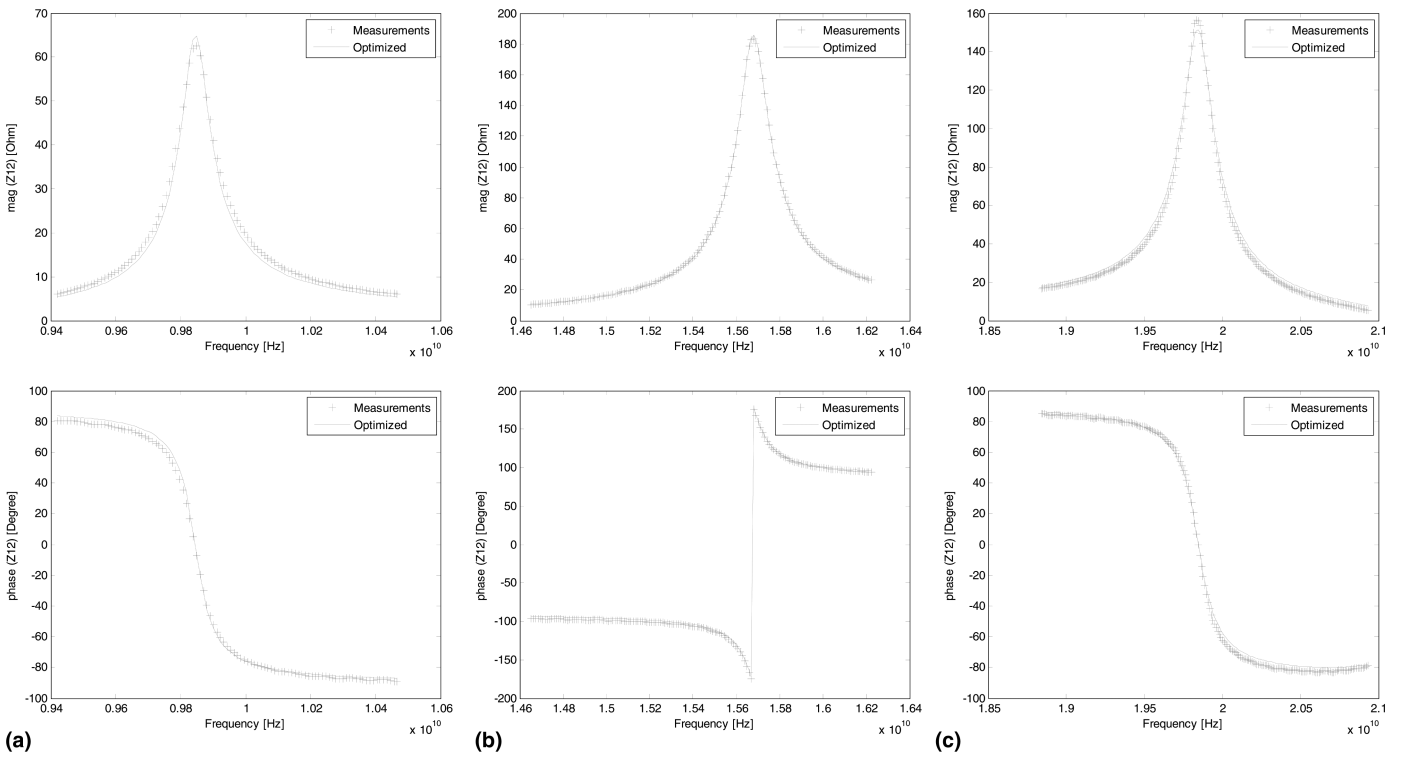


Fig. 5. Small resonator (278 mil × 278 mil): Measurement results versus fitted simulations at (a) the first, (b) the second, and (c) the third resonance frequencies. Nominal value used:  $\epsilon_r = 9$ ,  $\tan\delta = 0.002$ . Extracted values are shown in Fig. 6.

tangent extraction is only possible if the conductor losses are accurately modeled. The effect of surface roughness was included in our approach with the correction factor  $k$  based on the Hammerstadt formula as

$$k = 1 + \frac{2}{\pi} \tan^{-1} \left[ 1.4 \left( \frac{\Delta}{\delta} \right)^2 \right] \quad (3)$$

where  $\Delta$  is the rms value of surface roughness and  $\delta$  is the skin depth. An effective conductivity was used in simulations based on this correction factor as

$$\sigma_{\text{eff}} = \frac{\sigma_c}{k^2} \quad (4)$$

The nominal value chosen in the tracking sensitivity algorithm for the dielectric constant was 9.0, and loss tangent was 0.002. The order of the model for the rational approximation was chosen as 7. Using the automated method, the curve fitting

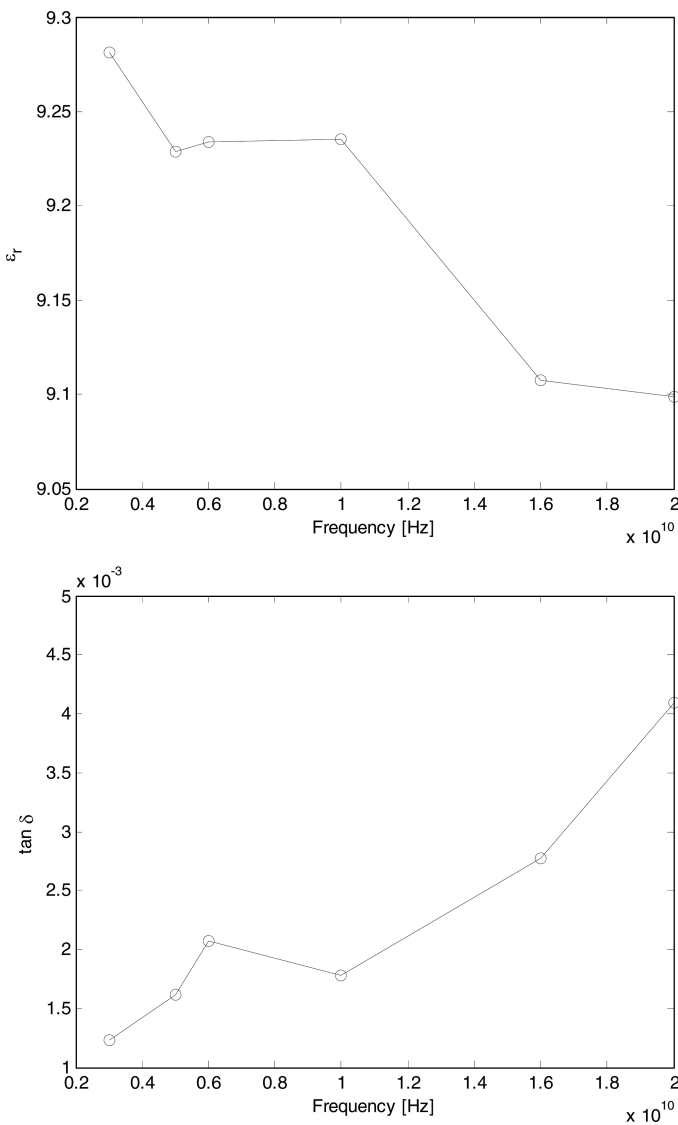


Fig. 6. Extracted dielectric constant and loss tangent of the ceramic substrate based on fitting the simulation to measurements as shown in Fig. 4 and Fig. 5.

resulted in a very good match to measured data as shown in Fig. 4 and Fig. 5. The agreement between simulated and measured data are very good.

Finally, Fig. 6 shows the extracted values for dielectric constant and loss tangent based on fitting simulations to measurements. Note that unlike analytical methods based on the Q-factor, the presented approach can be used to extract data not only at the first resonance frequency, but at the first 3-5 resonance frequencies. For broadband characterization, resonators of different sizes can be used as in the given example. Data were however not collected at identical frequencies from both resonators, as the first resonance frequency of the small resonator (at around 10 GHz) was larger than the fifth resonance frequency of the large resonator.

## CONCLUSION

In this paper, we presented a new automated method to extract the frequency-dependent dielectric constant and loss tangent of lossy substrates. This method is based on overlapping simulations with measurements for a cavity resonator.

To automate this curve-fitting problem in an efficient way, we introduced the tracking sensitivity algorithm, which provides an approximation of the simulated data as a low-order rational function of the complex permittivity. Hence, the iterative processes during curve-fitting can be computed very efficiently.

The automated method was applied on the extraction of the dielectric constant and loss tangent of HTCC ceramic. We also modeled the surface roughness loss for accurate extraction of the loss tangent. This new method is based on the measurements of a very simple test structure, and requires minimum information input by the user. Hence, we believe it will be useful in automated characterization of frequency-dependent dielectric constant and loss tangent of ceramic and organic substrates.

## ACKNOWLEDGMENTS

The authors would like to thank Dr. Jerry Aguirre from Kyocera USA for the fabricated ceramic resonators.

## REFERENCES

- [1] A. Deutsch, T.-M. Winkel, G. Kopcsay, C. Surovic, B. Rubin, G. Katopis, B. Chamberlin, and R. Krabbenhoft, "Extraction of  $\epsilon_r(f)$  and  $\tan\delta(f)$  for printed circuit board insulators up to 30 GHz using the short-pulse propagation technique," *IEEE Transactions on Advanced Packaging*, Vol. 28, No. 1, pp. 4-12, 2005.
- [2] Z. Zhou and K. Melde, "A comprehensive technique to determine the broadband physically consistent material characteristics of microstrip lines," *IEEE Transactions on Microwave Theory and Techniques*, Vol. 58, No. 1, pp. 185-194, 2010.
- [3] S. Yamacli, C. Ozdemir, and A. Akdagli, "A method for determining the dielectric constant of microwave PCB substrates," *International Journal of Infrared and Millimeter Waves*, Vol. 29, No. 2, pp. 207-216, 2008.
- [4] J. Rautio and S. Arvas, "Measurement of planar substrate uniaxial anisotropy," *IEEE Transactions on Microwave Theory and Techniques*, Vol. 57, No. 10, pp. 2456-2463, 2009.
- [5] X. Fang, D. Linton, C. Walker, and B. Collins, "Dielectric constant characterization using a numerical method for the microstrip ring resonator," *Microwave and Optical Technology Letters*, Vol. 41, No. 1, pp. 14-17, 2004.
- [6] J.-M. Heinola and K. Tolsa, "Dielectric characterization of printed wiring board materials using ring resonator techniques: A comparison of

- calculation models," *IEEE Transactions on Dielectrics and Electrical Insulation*, Vol. 13, No. 4, pp. 717-726, 2006.
- [7] R.K. Hoffmann, "*Handbook of Microwave Integrated Circuits*," Artech House Microwave Library, London, 1987.
- [8] A. Djordjevic, R. Biljic, V. Likar-Smiljanic, and T. Sarkar, "Wideband frequency-domain characterization of FR-4 and time-domain causality," *IEEE Transactions on Electromagnetic Compatibility*, Vol. 43, No. 4, pp. 662-667, 2001.
- [9] J. Howell, "A quick accurate method to measure the dielectric constant of microwave integrated-circuit substrates (short papers)," *IEEE Transactions on Microwave Theory and Techniques*, Vol. 21, No. 3, pp. 142-144, 1973.
- [10] A.E. Engin, "Extraction of dielectric constant and loss tangent using new rapid plane solver and analytical debye modeling for printed circuit boards," *IEEE Transactions on Microwave Theory and Techniques*, Vol. 58, No. 1, pp. 211-219, 2010.
- [11] D.E. Zelenchuk, V. Fusco, G. Goussetis, A. Mendez, and D. Linton, "Millimeter-wave printed circuit board characterization using substrate integrated waveguide resonators," *IEEE Transactions on Microwave Theory and Techniques*, Vol. 60, No. 10, pp. 3300-3308, 2012.
- [12] N. Biunno and I. Novak, "Frequency domain analysis and electrical properties test method for PCB dielectric core materials," Proceedings of DesignCon 2003 East, 2003.
- [13] "Non-destructive full sheet resonance test for permittivity of clad laminates," Standard IPC-TM-650, 2.5.5.6. The Institute for Interconnecting and Packaging Electronic Circuits, Bannockburn, IL, 1989.
- [14] A. Deutsch, A. Huber, G. Kopsay, B. Rubin, R. Hemedinger, D. Carey, W. Becker, T.-M. Winkel, and B. Chamberlin, "Accuracy of dielectric constant measurement using the full-sheet-resonance technique IPC-TM-650 2.5.5.6." Proceedings of the Conference on Electrical Performance of Electronic Packaging, pp. 311-314, 2002.
- [15] A.E. Engin, A. Tambawala, M. Swaminathan, P. Pramanik, and K. Yamazaki, "Causal modeling and extraction of dielectric constant and loss tangent for thin dielectrics," Proceedings of the IEEE International Symposium on Electromagnetic Compatibility, 2007.
- [16] Z. Guo, G. Pan, S. Hall, and C. Pan, "Broadband characterization of complex permittivity for low-loss dielectrics: Circular pc board disk approach," *IEEE Transactions on Antennas and Propagation*, Vol. 57, No. 10, pp. 3126-3135, 2009.
- [17] A. Engin, "An arnoldi algorithm for power-delivery networks with variable dielectric constant and loss tangent," *IEEE Transactions on Electromagnetic Compatibility*, Vol. 52, No. 4, pp. 859-865, 2010.
- [18] P. Pasunoori and A.E. Engin, "Automated dielectric constant and loss tangent characterization using cavity resonators," IEEE International Symposium on Electromagnetic Compatibility, 2011, EMC 2011, 2011.